Journal of Electrical and Computer Engineering Innovations
(JECEI)
Journal homepage: http://www.jecei.sru.ac.ir

Research paper

Modeling Transport in Graphene-Metal Contact and Verifying Transfer Length Method Characterization

B. Khosravi Rad[1], M. khaje[2], A. Eslami Majd[2,*]

[1]*Optoelectronics and Nanophotonics Research Group, Faculty of Electrical and Computer Engineering, Tarbiat Modares University, Tehran, Iran.*

[2]*Research electronic center, Malek Ashtar University of Technology, Tehran, Iran.*

Article Info

Article History:
Received 25 November 2022
Reviewed 10 January 2023
Revised 31 January 2023
Accepted 09 March 2023

Keywords:
Graphene-metal contact
Contact resistance
Transfer length method
Circuit modeling
Effective channel width

*Corresponding Author's Email Address: *a_eslamimajd@mut-es.ac.ir*

Abstract

Background and Objectives: One of the common methods for measuring the contact resistance of graphene sheets is the transfer length or transmission line method (TLM). Apart from the contact resistance, TLM gives the resistance of the channel sheet and the effective transfer length of the measured samples. Furthermore, the implementation of TLM is simple. To analyze this method, one can use circuit modeling (CM).

Methods: An important parameter of TLM is the contact resistance between the metal electrode and the graphene channel. To compare this parameter with other measures, it is normalized by multiplying it by the channel width. In this research, for TLM analysis, all the components of the structure including electrodes, graphene channel, and metal-graphene contact are modeled in a circuit.

Results: PSpice and MATLAB are integrated for TLM circuit modeling. The metal electrodes and the graphene channel are modeled based on the values of the resistances measured in the laboratory using the van der Pauw method and the resistances reported in the article in ohms per square. Moreover, the metal-graphene contact resistance is considered based on the values reported in the literature in ohms-micrometers.

Conclusion: The modeling results show that, in addition to the effective transfer length, the effective transfer width can be defined on a contact, according to the dimensions of the structure. Therefore, the channel width is a vague characteristic of the TLM measurement, which plays a very important role in measuring contact resistance. Furthermore, the contact resistance and the resistance of the channel sheet are independent of each other and of the distance between the contacts. If defects in the graphene channel are randomly distributed along the channel between the contacts, they do not have a significant impact on the contact resistance, while they increase the resistance of the graphene sheet provided that they do not disrupt the channel. Indeed, for a 10% defect (or 90% coverage along the channel), the resistance of the sheet increases by 16%. In addition, by using this modeling, parameters such as the distribution of the contact current, the sources of errors, and their influence in determining the contact resistance and resistance of the channel sheet are investigated.

Introduction

Contact resistance is one of the main limiting factors in the performance of short-channel graphene-based transistors [1]. The performance of an RF transistor is characterized by two parameters, the cut-off frequency (f_T) and the maximum oscillation frequency (f_{max}), which respectively represent the frequencies at which the current and power gain are unity and modulated by the gate; the cutoff frequency is obtained in (1), [2], [3], [4].

$$f_T = \frac{g_m}{2\pi c_g} \tag{1}$$

where Cg is the gate capacitance, and g_m is the conductivity. As a geometric parameter of field-effect transistors, the cutoff frequency has an inverse relationship with the square of the gate length and is almost independent of the width of the transistor. [2]. Nevertheless, better performance is observed in graphene transistors with much longer gate lengths, compared to Si and elements in groups 3 and 5 of the periodic table. Moreover, higher values of cutoff frequency have been reported for graphene transistors. Another important parameter in the RF transistors is f_{max}, which is indicated in (2) [5].

$$f_{max} = \frac{f_T}{\sqrt{\left(g_D\left(R_G + R_{SD}\right) + 2\pi f_T R_G C_G\right)}} \tag{2}$$

where g_D is the channel conductivity, R_G is the gate resistance, and R_{SD} is the drain-source resistance. Some studies have demonstrated that there is a significant difference between the values of f_T and f_{max} values in graphene RF transistors. To increase f_T, the carrier mobility should be increased [5], and three factors should be investigated and optimized: 1- the defects that depend on the growth process in graphene, 2- the impurities that cause scattering at the interface between the gate dielectric and graphene channel, and 3- contact resistance [3].

The frequency performance of graphene is limited by two factors, that is, the mobility of carrier in the graphene channel and the contact resistance of graphene-metal. The mobility of carrier in devices with a large channel length is dominant relation to the contact resistance. However, when the length of the channel is reduced, the role of the contact resistance in improving the speed of the device becomes critical and dominant [6]. Therefore, to improve the performance of graphene devices at high frequencies, the contact resistance in short-channel devices should be reduced as much as possible because the increase in contact resistance reduces the cutoff frequency [7], [8], [9]. A very important point is to characterize the metal-graphene contact resistance that can be made in several ways one of which is the TLM measurement [10], [11], [12], [13], [14]. In this method, important parameters, such as transmission length, contact resistance, and channel sheet resistance, are obtained [15], [16], [17], [18]. Then, each of the mentioned parameters is varied under the influence of different factors, such as contamination of the metal-graphene interface, defects or the presence of pollution particles in the graphene channel [19], and metal-graphene geometry, especially at the interface [20].

To better understand the transmission line method, TLM circuit modeling can be used. In this method, choosing geometric and physical values in appropriate ranges for metal-graphene contact helps to determine the limitations of the measurement method and provide correction coefficients for the measured values. In 2014, Vincenzi Giancarlo et al. investigated the contact current crowding or current transfer length (L_t) in circuit diagrams [21]. furthermore, in 2015, Zhang Peng et al. investigated the contact current crowding and its relationship with specific contact resistance. These authors demonstrated that the transfer length increases with the increase in the specific contact resistance [22]. In 2017, González-Díaz et al. also used a sample with a sheet resistance of 1 kΩ/□ (1kilo ohm/square) in a circuit model and evaluated the sources of error caused by finite size contacts in the van der Pauw measurement method [23]. The structure of TLM includes metal electrodes and a channel between them. The distances between the electrodes, or, the length of the channel, increase in an ascending manner. In TLM, by measuring the resistance between adjacent electrodes and plotting a graph of the obtained values, according to the distances between the contacts, the importance of contact resistance, transfer length, and sheet resistance are obtained. In practice, the TLM measurement method is used for graphene, as shown in Fig. 1. The measurement accuracy increases by increasing the number of contacts and changing the dimensions.

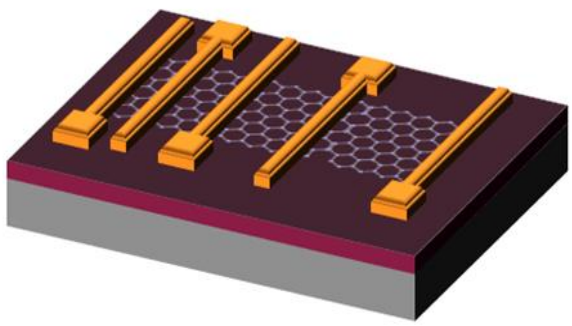

Fig. 1: Schematic of TLM measurement method.

The simple and one-dimensional circuit model of metal-graphene contact has been discussed in Refs. [24], [25], [26], [27] are shown in Fig. 2. As it is evident, these articles have only referred to the current distribution under the contact or the effective transfer length of the electrode.

In the present study, for the first time, the circuit model of the metal-graphene contact, in other words, the TLM method is simulated in three dimensions. Using the mentioned model, sources of error, current distribution under the contact, and an estimate of the effective transfer length and its relationship with the dimensions of the structure are discussed and analyzed. Also, the accuracy or inaccuracy of the model is analyzed. In addition to the mentioned cases, for the first time, the effective width of the channel is also checked, representing the part of the width of the graphene channel where the maximum amount of current enters it. The current entering the graphene channel from the metal electrode, instead of uniformly covering the entire channel, the part of the channel closer to the current source contributes more to the current flow. In other words, the electric current chooses the shortest path to pass.

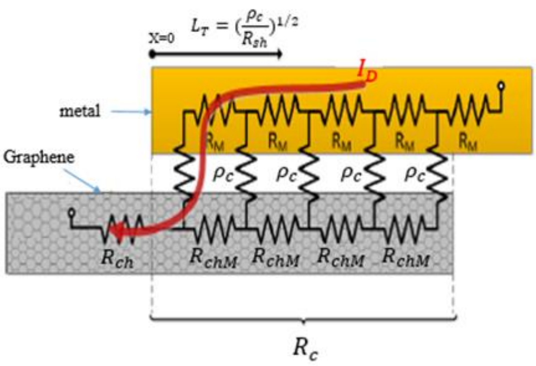

Fig. 2: One-dimensional circuit model of metal-graphene contact.

Results and Discussion

The transfer length method includes metal electrodes, the substrate, the channel between the electrodes, and the contact resistance between them. A network of electrical resistances models the graphene sheet and metal electrodes in a circuit form. To model the graphene channel and metal contacts, a square unit cell is considered whose dimensions are the same as those of the graphene channel and metal electrodes. Then, each unit cell of metal contacts and graphene channel is modeled independent of the dimensions of the unit cell, using four resistors with values of $2R_{shm}$ and $2R_{shG}$, respectively (see Fig. 3). In this model, the resistances of the channel and metal sheet (R_{shm} and R_{shG}) are expressed in ohm/square.

Table 1: TLM modeling parameters

Measurement parameters	Unit	Values
Contact length (L_C)	µm	1
Channel width (w)	µm	5
Contact distances (d)	µm	1, 2, 3, 4, 5, 6
Channel sheet resistance (R_{shG})	Ω/□	500
Metal sheet resistance (R_{shm})	Ω/□	5
Contact resistance (R_C)	Ω.µm	200

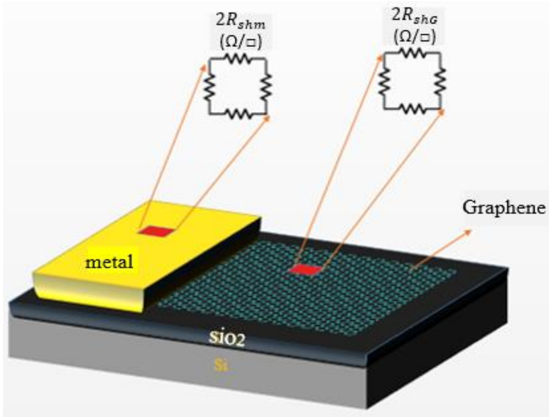

Fig. 3: Circuit schematic of metal electrode and graphene channel.

After determining the dimensions of the channel and metal electrodes, they are modeled using PSpice according to Fig. 4. This figure shows Ni metal electrodes with a sheet resistance of 5 Ω/□ corresponding to 20 nm of the metal, which is measured using the van der Pauw method. Also, the sheet resistance of monolayer graphene, with a thickness of 0.34nm, is considered 500 Ω/□. This value is based on the values obtained from the van der Pauw measurement method carried out on the CVD graphene transferred on a SiO_2/Si substrate in the laboratory. In addition, the contact resistance at the metal-graphene interface is modeled with a value of 200 Ω.µm according to the literature (e.g., see Refs. [18], [28], [29], [30], [31] that report values in the range of 100-2500 Ω.µm). In this case, the normalized contact resistance values per micron are used. As shown in Fig. 4, the dimensions of metal contacts and graphene channels are small, so the expansion of the mentioned structure using PSpice is very time-consuming and challenging. Then, for more flexibility and the ability to change the system of TLM, the netlist related to the resistances of metal electrodes, graphene channel, and contact resistances, along with the contacts between them, was produced by MATLAB. The generated netlist was executed in PSpice, and its results were checked.

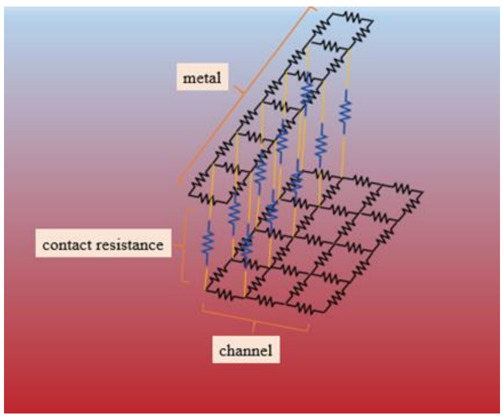

Fig. 4: Circuit modeling of the metal electrode, graphene channel, and contact resistance.

Finally, the TLM diagram was plotted, as shown in Fig. 5. This figure's results confirm the model's correctness.

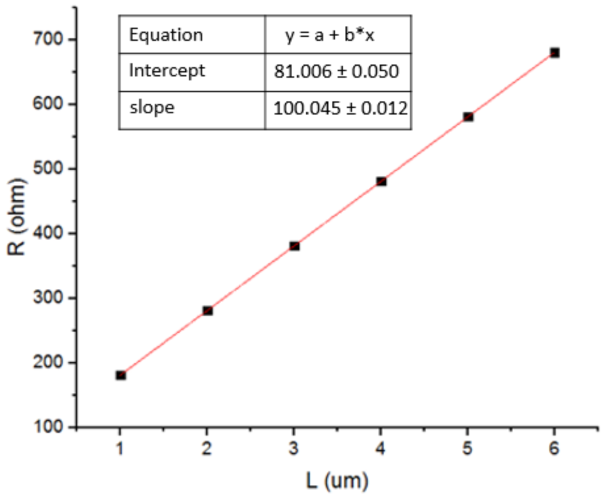

Fig. 5: TLM measurement diagram for graphene in circuit modeling mode.

Another parameter evaluated in this study is the transfer length of the metal electrode. To extract this parameter and show the current distribution under the contact, the dimensions in Table 1, with a 2 µm increase in the electrode length, a 10 µm increase in the channel width, and a channel length of 1 µm, were considered. Then, the results of the current distribution under the contact were obtained, as shown in Fig. 6. The horizontal and vertical axes represent the length of the metal electrode and the width of the channel, respectively. Here, the current distribution under the contact and the effective length of the metal electrode are involved in the transfer.

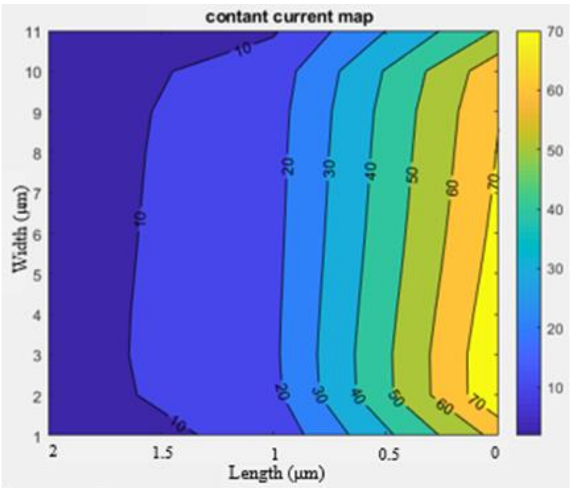

Fig. 6: Current distribution from the metal electrode to the graphene channel. The maximum current is transferred along less than 1 µm of the metal electrode.

A. Effect of Channel Width on the Accuracy of Measuring Contact Resistance and Channel Sheet Resistance

After examining the transfer length parameter, the effect of channel width (w) on the measurement of contact resistance and sheet resistance was investigated for a fixed channel length. In this case, the modeling based on the TLM measurement method was used for different widths of the graphene sheet, and the results are shown in Table 2. These results indicated that from one point on, if the entire width of the channel is applied to normalize contact resistance, the measurement error increases, and contact resistance becomes more significant than the desired value in the modeling. It was found that by increasing the, instead of the entire width of the channel, only a part of it participates in the current transfer. In other words, a part of the channel width significantly contributes to the current transfer. The reason for this phenomenon can be the resistance of the metal sheet on the graphene channel, which depends on the type of metal and the sheet thickness. To solve this problem, the graphene channel's width and, consequently the electrode's dimensions should be reduced as much as possible so that the passing current has a shorter path to flow. Also, the thickness of the metal sheet should be such that its resistance is low. suppose the resistance of the metal electrode and channel width is small, instead of taking a shorter path for entering the channel. In that case, the current can flow throughout the metal electrode and then enter the channel uniformly. In this case, the effective width of the channel is equal to the width of the channel.

Table 2: Effective widths obtained for different channel widths

Channel width (w, µm)	effective channel width (w_{ef}, µm)	Model contact resistance (R_C.w, Ω.µm)	Measured contact resistance (R_C.w, Ω.µm)
5	4.94	200	202.5
6	5.6	200	214.35
7	5.98	200	234.15
8	6.3	200	254
9	6.52	200	276.3
10	6.7	200	299

To show the current distribution across the width of the channel, the dimensions of the contacts and the channel were considered according to Table 3. The results in terms of different widths (w) are shown in Fig. 7. From this figure, for a width greater than 20 µm, the uniformity of the current distribution across the width of the channel starts to change. Also, this issue was investigated, for different values of the metal sheet resistance, and it was shown that the values of metal sheet resistance, which depend on the thickness of the metal sheet, affect the mentioned results. Therefore, if the structure dimensions are not carefully considered, an error can occur in the normalized values of the metal-graphene contact resistance.

Table 3: Parameters for plotting the effective width of the channel

Measurement parameters	Unit	Values
L_C	µm	2
w	µm	20, 30, 40, 50
d	µm	10
R_{shG}	Ω/□	500
R_{shm}	Ω/□	5
R_C	Ω.µm	200

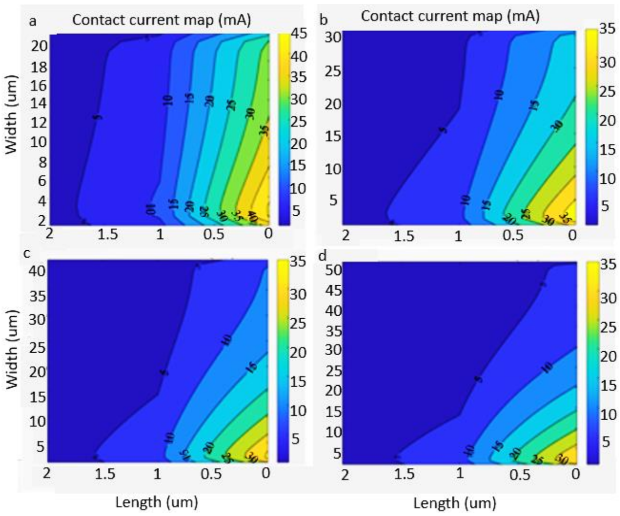

Fig. 7: Current distribution from the metal to the graphene channel. (a) The channel width is 20 µm. (b) The channel width is 30 µm. (c) The channel width is 40 µm. (d) The channel width is 50 µm.

B. Effect of Distances Between Contacts and Channel Defects on Measuring Channel Sheet and Contact Resistances

The TLM measurement method was modeled to investigate the effect of the distances between electrodes or the length of the channel in the measurement of contact resistance. The results were plotted for different distances between the contacts. In this case, the channel is uniform and homogeneous. According to Fig. 8, the contact and channel sheet resistance values are the same for different channel dimensions.

However, when 10% of defects are considered for the graphene channel, the TLM measurement diagram (Fig. 9) shows that the contact resistance decreases by a few percent compared to the defect-free state, which is not very noticeable, while the channel sheet resistance increases by 16%.

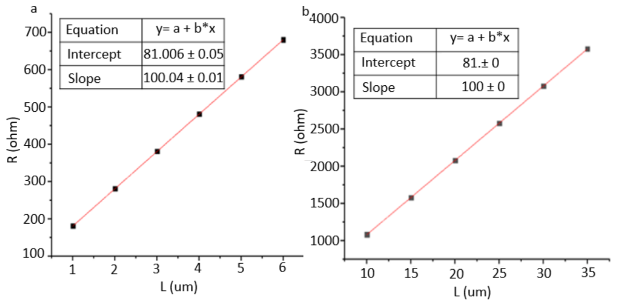

Fig. 8: TLM measurement diagram for distances of (a) 1, 2, 3, 4, 5, 6 and (b) 10, 15, 20, 25, 30, and 35 microns between electrodes.

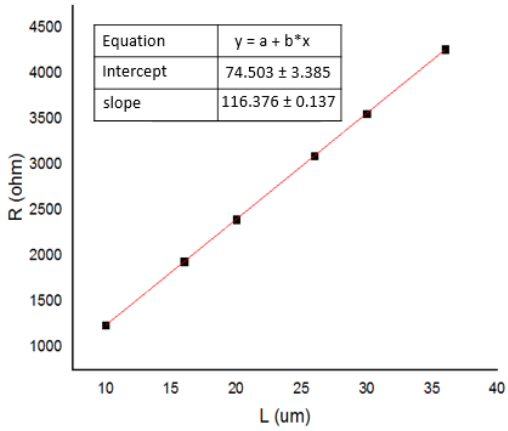

Fig. 9: TLM measurement diagram for 10% defects in the channel and inter-contact distances of 10, 16, 20, 26, 30, and 36 µm; channel sheet resistance has increased by 16%.

When the graphene channel defect is 20%, the contact resistance is almost unchanged, but the channel sheet resistance increases by 32% (Fig. 10). Therefore, it can be concluded that if the defect is spread throughout the graphene sheet or the area between the electrodes (provided that it does not interrupt the channel), then the contact resistance remains almost constant while the channel sheet resistance increases.

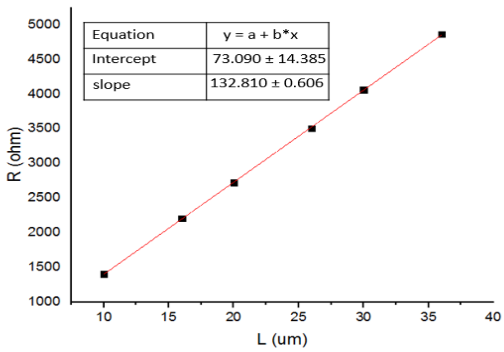

Fig. 10: TLM measurement diagram for 20% defects in channel and inter-contact distances of 10, 16, 20, 26, 30, and 36 µm; channel sheet resistance has increased by 32%.

C. Effect of Error in Measuring Distances Between Electrodes on Contact Resistance and Channel Sheet Resistance

Other parameters affecting the TLM measurement results are relative errors in measuring the distances between contacts and their resistances. Therefore, the TLM diagram was plotted by assuming an error of 5% in the measurement of distances between the contacts for contact distances of 10, 15, 20, 25, 30, and 35 micrometers. According to Fig. 11, the error in measuring of distances between the contacts does not affect the value of the contact resistance, but it changes the channel sheet resistance.

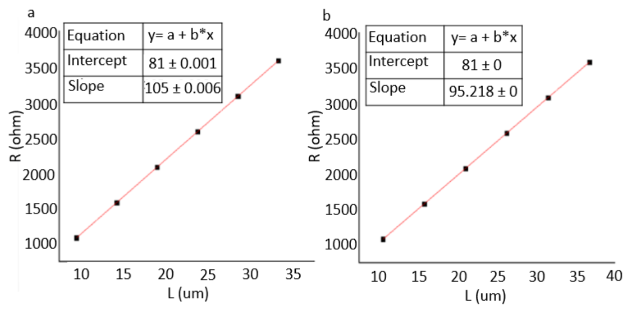

Fig. 11: TLM diagram for 5% error in measuring the distances between contacts for distances of (a) 9.5, 14.25, 19, 23.75, 28.5, 33.25 and (b) 10/5, 15/75, 21, 26/25, 31/5, 36/75 microns.

D. Effect of Error in Measuring the Resistance Between Contacts on Metal-Graphene Contact Resistance and Graphene Sheet Resistance

In this case, assuming an error of 5% in measuring the resistance between the electrodes, the contact and channel sheet resistance values show a 5% error (see Fig. 12). If the error rate is added to the measured resistance values between the electrodes, these parameters increase by 5%. Otherwise, the same amount of error is obtained again for contact and channel sheet resistance, with the difference that their values are reduced this time.

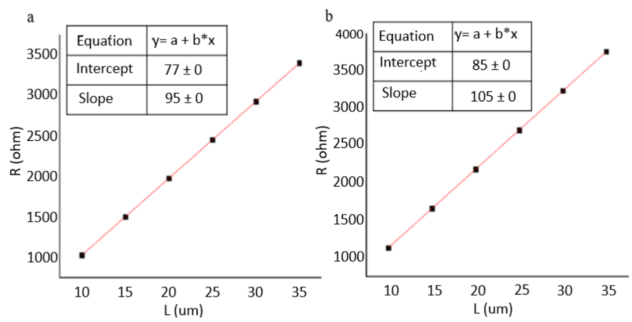

Fig. 12: TLM measurement diagram for 5% error in measuring the resistance between metal electrodes. The error percentage has (a) been summed with and (b) subtracted from the actual value of the measured resistances.

E. Proposing TLM Structure and Providing Channel Width Correction Coefficients

It was considered that the normalized resistance of the contact depends on the dimensions of the TLM structure and the channel width. Therefore, a structure with specific dimensions and appropriate correction coefficients was presented. In this structure, the metal sheet resistance was considered 3 Ω/□, obtained using the van der Pauw measurement method for a thickness of 30 nm of Ni metal sheet. Other characteristics of the structure are shown in Table 4.

Table 4: Modeling parameters of the proposed TLM structure

Measurement Parameters	Unit	Values
L_C	µm	2
w	µm	20, 30, 40, 50
d	µm	10
R_{shG}	Ω/□	500
R_{shm}	Ω/□	5
R_C	Ω.µm	200

By comparing the values obtained from the measurement diagram with the values from modeling, the correction coefficients are determined according to Table 5. These coefficients are obtained by dividing the modeling contact resistance by the measured contact resistance.

Table 5: Correction coefficients for measured contact resistance

Modeling contact resistance (Ω.µm)	Modeling channel width (µm)	Measured contact resistance (Ω.µm)	Correction coefficients
100	10	166.5	0.601
200	10	264.2	0.760
300	10	363.5	0.825
400	10	466	0.859
500	10	576.5	0.867

Conclusion

In this article, for the first time, circuit modeling of the TLM method has been done, and by using this modeling, parameters such as current distribution under the contact, effective transfer length, error sources, and~~,~~ their influence in determining the contact resistance and channel sheet resistance have been investigated. The modeling showed that the maximum current is transferred in a length of fewer than 1 µm of the metal electrode. Most importantly, it has been shown for the first time that in addition to the effective transfer length, the effective channel width, which plays a vital role in determining the normalized contact resistance and channel sheet resistance, is an ambiguous aspect of the TLM measurement method that has not been mentioned so far. It was found that by increasing the width of the channel, only a part of it participates in the current transfer. In other words, a part of the channel width significantly contributes to the current transfer. The reason for this phenomenon can be the resistance of the metal sheet on the graphene channel, which depends on the type of metal and the sheet thickness. In addition, it was shown that the measurement of the contact and channel sheet resistance are independent of each other and the distances between electrodes. Furthermore, the contact resistance is almost constant for the defects in the graphene channel, but the channel sheet resistance increases. The effect of the error in measuring the distances/resistances between the contacts on the contact resistance and channel sheet resistance was investigated. The error in the measurement of spaces between the contacts does not affect the value of the contact resistance, but it changes the channel sheet resistance. However, the error in measuring the resistance between the electrodes causes the values of the contact resistance and the channel sheet resistance to change by the same amount of error.

Author Contributions

All the authors participated in the conceptualization and implementation, and B. Khosravi Rad wrote the manuscript.

Acknowledgment

The authors would like to acknowledge the Faculty of Electrical & Computer Engineering, Malek Ashtar University of Technology, and the Microelectronic laboratory, for their support and contribution to this study.

Conflict of Interest

The authors declare no potential conflict of interest regarding the publication of this work. In addition, the ethical issues including plagiarism, informed consent, misconduct, data fabrication and, or falsification, double publication and, or submission, and redundancy have been completely witnessed by the authors.

Abbreviations

TLM	Transfer Length Method
CM	Circuit Modeling
ETL	Effective Transfer Length
CR	Contact Resistance
CSR	Channel Sheet Resistance
ETW	Effective Transfer width
MSR	Metal Sheet Resistance

References

[1] L. Anzi et al., "Ultra-low contact resistance in graphene devices at the Dirac point," 2D Mater., 5(2): 025014, 2018.

[2] Y. M. Lin et al., "Development of graphene FETs for high frequency electronics," in Proc. 2009 IEEE International electron devices Meeting (IEDM): 1-4, 2009.

[3] K. Kim, J. Y. Choi, T. Kim, S. H. Cho, H. J. Chung, "A role for graphene in silicon-based semiconductor devices," Nature, 479(7373): 338-344, 2011.

[4] J. Zheng et al., "Sub-10 nm gate length graphene transistors: operating at terahertz frequencies with current saturation," Sci. Rep., 3(1): 1-9, 2013.

[5] W. Zhu et al., "Graphene radio frequency devices on flexible substrate," Appl. Phys. Lett., 102(23): 233102, 2013.

[6] Y. Wu et al., "High-frequency, scaled graphene transistors on diamond-like carbon," Nature, 472(7341): 74-78, 2011.

[7] M. R. Islam, M. A. Haque, M. Fahim-Al-Fattah, M. N. K. Alam, M. R. Islam, "Dynamic performance of graphene field effect transistor with contact resistance," in Proc. 2016 5th International Conference on Informatics, Electronics and Vision (ICIEV): 21-25, 2016.

[8] Y. Wu et al., "RF performance of short channel graphene field-effect transistor," in Proc. 2010 International Electron Devices Meeting: 9.6.1-9.6.3., 2010.

[9] A. Mehrfar, A. Eslami Majd, "Enhancement of the photoresponse in the platinum silicide photodetector by a graphene layer," J. Electr. Comput. Eng. Innovations (JECEI), 10(2): 363-370, 2022.

[10] D. K. Schroder, Semiconductor material and device characterization. John Wiley & Sons, 2015.

[11] V. Passi et al., "Contact resistance Study of “edge-contacted” metal-graphene interfaces," in Proc. 2016 46th European Solid-State Device Research Conference (ESSDERC): 236-239, 2016.

[12] B. K. Bharadwaj, D. Nath, R. Pratap, S. Raghavan, "Making consistent contacts to graphene: effect of architecture and growth induced defects," Nanotechnology, 27(20): 205705, 2016.

[13] A. Quellmalz et al., "Influence of humidity on contact resistance in graphene devices," ACS applied materials & interfaces, 10(48): 41738-41746, 2018.

[14] V. Passi et al., "Ultralow specific contact resistivity in metal–graphene junctions via contact engineering," Adv. Mate. Interfaces, 6(1): 1801285, 2019.

[15] J. Anteroinen, W. Kim, K. Stadius, J. Riikonen, H. Lipsanen, J. Ryynanen, "Extraction of graphene-titanium contact resistances using transfer length measurement and a curve-fit method," Int. J. Mate. Metall. Eng., 6(8): 807-810, 2012.

[16] J. Moon et al., "Ultra-low resistance ohmic contacts in graphene field effect transistors," Appl. Phys. Lett., 100(20): 203512, 2012.

[17] F. Giubileo, A. Di Bartolomeo, "The role of contact resistance in graphene field-effect devices," Prog. Surf. Sci., 92(3): 143-175, 2017.

[18] A. Gahoi, S. Wagner, A. Bablich, S. Kataria, V. Passi, M. C. Lemme, "Contact resistance study of various metal electrodes with CVD graphene," Solid-State Electron., 125: 234-239, 2016.

[19] S. Burzhuev, "Decreasing Graphene Contact Resistance by Increasing Edge Contact Length," University of Waterloo, 2016.

[20] M. Houssa, A. Dimoulas, A. Molle, 2D materials for nanoelectronics. CRC Press, 2016.

[21] G. Vincenzi, "Graphene: FET and Metal Contact Modeling. Graphène: modélisation du FET et du contact métallique," Université Paul Sabatier-Toulouse III, 2014.

[22] P. Zhang, Y. Lau, R. Gilgenbach, "Analysis of current crowding in thin film contacts from exact field solution," J. Phys. D: Appl. Phys., 48(47): 475501, 2015.

[23] G. González-Díaz et al., "A robust method to determine the contact resistance using the van der Pauw set up," Measurement, 98: 151-158, 2017.

[24] F. Liu, W. T. Navaraj, N. Yogeswaran, D. H. Gregory, R. Dahiya, "van der Waals contact engineering of graphene field-effect transistors for large-area flexible electronics," ACS nano, 13(3): 3257-3268, 2019.

[25] K. A. Jenkins, "Graphene in high-frequency electronics: This two-dimensional form of carbon has properties not seen in any other substance," Am. Sci., 100(5): 388-398, 2012.

[26] F. Urban, G. Lupina, A. Grillo, N. Martucciello, A. Di Bartolomeo, "Contact resistance and mobility in back-gate graphene transistors," Nano Express, 1(1): 010001, 2020.

[27] P. Zhang, Y. Lau, "An exact field solution of contact resistance and comparison with the transmission line model," Appl. Phys. Lett., 104(20): 204102, 2014.

[28] W. S. Leong, H. Gong, J. T. Thong, "Low-contact-resistance graphene devices with nickel-etched-graphene contacts," ACS nano, 8(1): 994-1001, 2014.

[29] K. Nagashio, T. Nishimura, K. Kita, A. Toriumi, "Contact resistivity and current flow path at metal/graphene contact," Appl. Phys. Lett., 97(14): 143514, 2010.

[30] A. Venugopal, L. Colombo, E. Vogel, "Contact resistance in few and multilayer graphene devices," Appl. Phys. Lett., 96(1): 013512, 2010.

[31] S. M. Popescu, A. J. Barlow, S. Ramadan, S. Ganti, B. Ghosh, J. Hedley, "Electroless nickel deposition: an alternative for graphene contacting," ACS Appl. Mate. Interfaces, 8(45): 31359-31367, 2016.

Biographies

Babak Khosravi Rad was born in khorramabad in iran, 1993. he received the B.Sc. degree in Electrical Engineering from lorestan University of Technology, Lorestan, Iran. Also, he received the M.Sc. degree in Electrical Engineering from Malek-Ashtar University of Technology and He is a Ph.D. student in electronics from Tarbiat Modares University, Tehran, Iran. His research interests include GFET, detector, MEMS, and semiconductor field effect devices.

• Email: khosravirad_babak@modares.ac.ir
• ORCID: NA
• Web of Science Researcher ID: NA
• Scopus Author ID: NA
• Homepage: NA

Mehdi Khaje received the M.Sc. and Ph.D. degree in Electrical Engineering from Malek-Ashtar and Orumiyeh University of Technology, respectively. His research interests include superconducting amplifying and detector devices, MEMS, and semiconductor field effect devices.

• Email: m.khaje@mut.ac.ir
• ORCID: NA
• Web of Science Researcher ID: NA
• Scopus Author ID: NA
• Homepage: NA

Abdollah Eslami Majd was born in Hamadan, Iran, on March 23, 1976. He received the B.E. degree in applied physics from bu-ali Sina University, Hamadan, Iran in 1998. He received M.E. degree in atomic and molecular physics from Amir kabir University of Technology Tehran Polytechnic, Tehran, Iran in 2001. He received the Ph.D. Degree in photonics from laser and plasma Institute of Shahid Beheshti University, Tehran, Iran in 2011. Since joining electrical engineering and electronic department of Malek Ashtar University of Technology in 2012, he has engaged in research and development of stary light in the satellite camera, laser induced breakdown spectroscopy (LIBS) and hemispherical resonator gyroscope (HRG). He is co-author of more than 30 publications. Dr. Eslami is a member of Optics and Photonics Society of Iran and Physics Society of Iran.

• Email: a_eslamimajd@mut-es.ac.ir
• ORCID: 0000-0002-7538-3160
• Web of Science Researcher ID: NA
• Scopus Author ID: NA
• Homepage: NA

How to cite this paper:
B. Khosravi Rad, M. khaje, A. Eslami Majd, “modeling transport in graphene-metal contact and verifying transfer length method characterization,” J. Electr. Comput. Eng. Innovations, 11(2): 335-362, 2023.

DOI: 10.22061/jecei.2023.9266.597

URL: https://jecei.sru.ac.ir/article_1841.html